Coumarin and Chromen-4-one Analogues as Tautomerase Inhibitors of Macrophage Migration Inhibitory Factor: Discovery and X-ray Crystallography

Masaya Orita,* Satoshi Yamamoto, Naoko Katayama, Motonori Aoki, Kazuhisa Takayama, Yoko Yamagiwa, Norio Seki, Hiroshi Suzuki, Hiroyuki Kurihara, Hitoshi Sakashita, Makoto Takeuchi, Shigeo Fujita, Toshimitsu Yamada, and Akihiro Tanaka

Yamanouchi Pharmaceutical Company Ltd., 21 Miyukigaoka, Tsukuba Science City 305-8585, Japan

Received September 5, 2000

Macrophage migration inhibitory factor (MIF) is a proinflammatory cytokine released from T-cells and macrophages. Although a detailed understanding of the biological functions of MIF has not yet been clarified, it is known that MIF catalyzes the tautomerization of a nonphysiological molecule, D-dopachrome. Using a structure-based computer-assisted search of two databases of commercially available compounds, we have found 14 novel tautomerase inhibitors of MIF whose K_i values are in the range of 0.038−7.4 μM. We also have determined the crystal structure of MIF complexed with the hit compound **1**. It showed that the hit compound is located in the active site of MIF containing the N-terminal proline which plays an important role in the tautomerase reaction and forms several hydrogen bonds and undergoes hydrophobic interactions. A crystallographic study also revealed that there is a hydrophobic surface which consists of Pro-33, Tyr-36, Trp-108, and Phe-113 at the rim of the active site of MIF, and molecular modeling studies indicated that several more potent hit compounds have the aromatic rings which can interact with this hydrophobic surface. To our knowledge, our compounds are the most potent tautomerase inhibitors of MIF. One of these small, drug-like molecules has been cocrystallized with MIF and binds to the active site for tautomerase activity. Molecular modeling also suggests that the other hit compounds can bind in a similar fashion.

Introduction

Macrophage migration inhibitory factor (MIF) is the first identified T-cell-derived soluble lymphokine. It was originally found to inhibit the random migration of macrophages and activate them at inflammatory loci.[1,2] However, recently, it was revealed that MIF is an anterior pituitary-derived hormone, potentiating lethal endotoxemia[3] and overriding the glucocorticoid-mediated suppression of inflammatory and immune responses;[4] it also plays an essential role in the activation of T-cells after mitogenic and antigenic stimuli.[5] More recent studies showed that anti-MIF antibody is therapeutically beneficial in a variety of animal models of proinflammatory diseases including sepsis,[3,6] adult respiratory disease syndrome,[7] rheumatoid arthritis,[8,9] glomerulonephritis,[10] and allograft rejection.[11] Gene deletion studies with mice also confirmed an important role for MIF in sepsis and lung inflammatory disease.[12] These findings indicate that MIF is a key molecule in inflammation and that its specific inhibitors may lead to an antiinflammatory therapeutic agent.

Several crystallographic studies of MIF revealed that the monomer of MIF consists of two antiparallel α-helices that are packed against a four-stranded β-sheet, and three monomers associate to form a symmetrical trimer which is joined by intersubunit β-sheets.[13−18] X-ray data also revealed that the three-dimensional structure of MIF is not similar to that of any known cytokine, but it is strikingly homologous to that of two other bacterial isomerases, 4-oxalocrotonate tautomerase (4-OT) and 5-carboxylmethyl-2-hydroxymuconate isomerase (CHMI), which catalyze the isomerization of unsaturated ketones.[19] Although the sequence alignment between MIF and these two enzymes shows relatively low homology (<20%), these enzymes are both homotrimers, as is MIF (OT is a trimer of a homodimer, and the OT homodimer is a structure similar to the monomers of CHMI and MIF), and the N-terminal proline which 4-OT and CHMI utilize as a catalytic base in the enzymatic reaction is also conserved in MIF.

Scheme 1

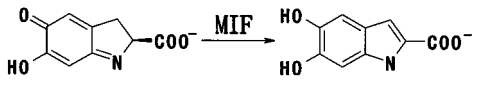

D-dopachrome DHICA

Recently, Rosengren et al. discovered during the study of melanin biosynthesis that MIF catalyzes a tautomerization reaction of D-2-carboxy-2,3-dihydroindole-5,6-quinone (D-dopachrome) to 5,6-dihydroxyindole-2-carboxylic acid (DHICA)[20] (Scheme 1), and they also reported that MIF catalyzes tautomerization of phenylpyruvate and *p*-hydroxyphenylpyruvate (HPP).[21] Interest in the relation between the biological activities of MIF and tautomerase activity has increased; however, their association has not been clarified and natural ligands for MIF also have not yet been identified. D-dopachrome is not a physiological molecule, and phenylpyruvate and HPP are thought not to be physiological substrates because of their separate localization from MIF and the kinetic parameters for the tautomerase reactions.[21]

* To whom correspondence should be addressed. Tel: 81-298-52-5111. Fax: 81-298-52-5387. E-mail: orita@yamanouchi.co.jp.

10.1021/jm000386o CCC: $20.00
Published on Web 12/30/2000

Several trials have been carried out to find MIF inhibitors in order to provide a validation tool in a chemical approach. Bucala et al. showed that dopachrome analogues inhibit the tautomerase activity of MIF[22] (the IC_{50} values of their compounds were in the range of 100−1000 μM), and recently, they discovered small molecules, tryptophan derivatives that inhibit the tautomerase activity of MIF.[23] The IC_{50} value of the most potent compound they found was 5.0 μM. Swope et al. reported that *S*-hexylglutathione binds to the active site of MIF with a K_d of 2.5 ± 0.6 mM, using NMR.[24] They also found that *S*-hexylglutathione and hexanethiol inhibit the tautomerase activity of MIF with IC_{50} values of 3.3 ± 1.6 mM and 17.4 ± 4.9 μM, respectively. Taylor et al. showed that a phenylpyruvate tautomerase inhibitor, (*E*)-2-fluoro-*p*-hydroxycinnamate, inhibits the tautomerase reaction of MIF with a K_i of 2.6 μM.[18]

A potent tautomerase inhibitor is expected to be a validation tool which can clarify the role of the enzymatic activity of MIF and the relation between its biological and enzymatic activity, and there is a possibility that a tautomerase inhibitor may be used for MIF-related disease. In this paper, we report the discovery of a novel tautomerase inhibitor of MIF, using a structure-based computer-assisted search. The inhibitor binding site was also examined by determining the crystal structure of MIF complexed with one of the hit compounds. The K_i values of our compounds are in the range of 0.038−7.4 μM. To our knowledge, our compounds are the most potent tautomerase inhibitors of MIF.

Results and Discussion

Structure-Based Computer-Assisted Search and Tautomerase Assay. Various docking methods using the three-dimensional structures of target proteins have been utilized for drug targets, and many discoveries of drug leads have been reported, especially in the field of enzyme inhibitors.[25,26,32−34] To identify a tautomerase inhibitor of MIF, a structure-based computer-assisted search in ACD and ACDSC was perfomed.

DOCK4.0.1[25,26] was used for searching about 1 000 000 compounds in ACD and ACDSC. During the process of selecting the compounds, we used not only simple scoring procedures in DOCK4.0.1 but also performed careful visual inspection. We also removed reagents, chemically unstable compounds, and compounds which did not satisfy the condition of the rule-of-5[27] using an in-house program. The rule-of-5, which was developed by Lipinski et al., is probably the best-known approach to predict the absorption of the compounds and is very useful for filtering out the compounds which were predicated to have an absorption problem from a large molecular database. Finally, we selected 524 compounds and purchased them for testing in the tautomerase inhibition assay of MIF.

The 524 compounds which were purchased from commercial suppliers were assayed without further purification. Fourteen hit compounds which showed K_i values below 10 μM were found, and the K_i value of the most potent compound was 38 nM. Some compounds which do not have double ring group, such as the benzene derivatives, were also selected in our virtual screening; however, their K_i values were above 100 μM. Other known MIF inhibitors, dophachrome analogues, and (*E*)-2-fluoro-*p*-hydroxycinnamate did not show up, because they are not included in the databases we used. The tryptophan derivatives which were found by Bucala et al. and hexanethiol were removed in the process of the selection of the compounds, though they were included in the databases, because they have chemically unstable imine and reactive thiol groups, respectively. *S*-Hexylglutathione, which is also included in the databases, did not show a good score in our virtual screening. It may be reasonable because its binding affinity is not strong (K_d value is 2.5 ± 0.6 mM). The structures of all hit compounds were confirmed by ^{1}H NMR, ^{13}C NMR, and HRMS. Figure 1 shows the structures of the 14 hit compounds, and Table 2 lists their K_i values.

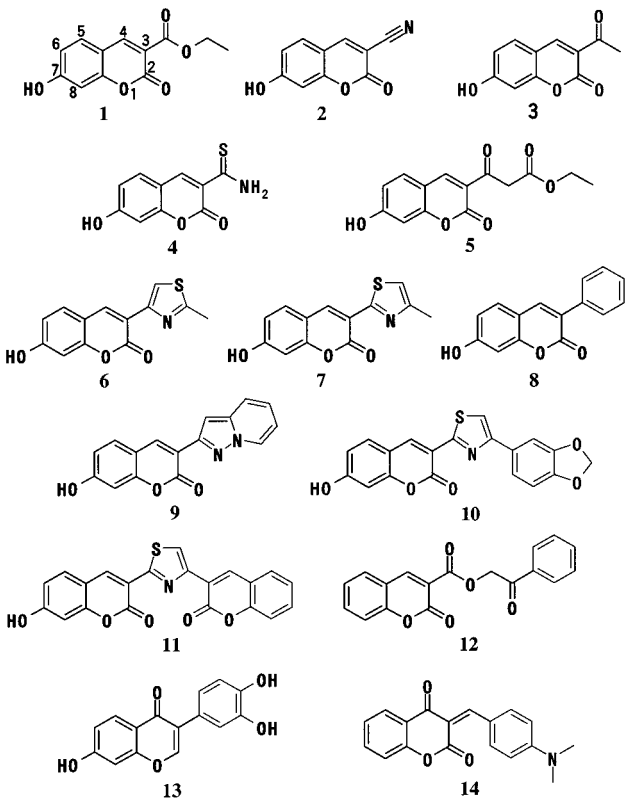

Figure 1. Structures of tautomerase inhibitors of MIF found by structure-based computer-assisted search in ACD and ACDSC.

Table 1. Crystallographic Data for the Free and Compound **1**-Inhibited Human MIF Crystals

	free form	inhibited form
space group	$P2_12_12_1$	$P2_12_12_1$
cell (Å)	a = 67.5, b = 67.5, c = 88.3	a = 67.6, b = 67.4, c = 87.3
molecules/asu	3	3
resolution (Å)	100−1.5	20−1.9
no. of unique reflns	566791 (>2σ)	27784 (>2σ)
completeness	86.9%	86.6%
R_{merge}	0.032	0.035
R_{work}	0.191	0.199
R_{free}	0.215	0.240
rms bond (Å)	0.013	0.014
rms angle (deg)	1.5	1.6

Determination of Crystal Structures. To examine the detailed interactions between MIF and our hit compounds, the X-ray structure of MIF complexed with compound **1** has been determined. Our crystallographic

Table 2. Inhibition Constants of 14 Hit Compounds

compd	K_i (μM)	compd	K_i (μM)	compd	K_i (μM)
1	7.4 ± 2.0	**6**	2.1 ± 0.15	**11**	0.28 ± 0.031
2	2.9 ± 0.44	**7**	3.1 ± 0.30	**12**	1.6 ± 0.29
3	4.3 ± 0.62	**8**	0.47 ± 0.041	**13**	0.038 ± 0.0046
4	0.55 ± 0.077	**9**	0.50 ± 0.049	**14**	6.2 ± 0.53
5	5.8 ± 0.54	**10**	1.5 ± 0.16		

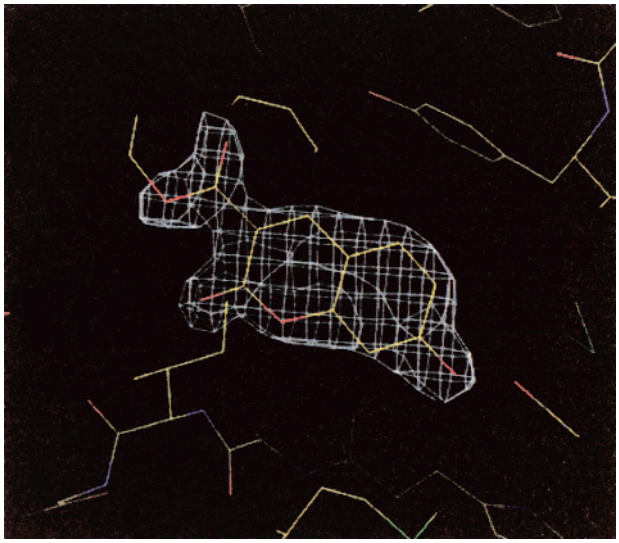

Figure 2. $F_o - F_c$ simulated annealing omit electron-density map (3.0σ) showing the bound compound **1** in the active site of MIF.

studies showed that the overall structures of both the ligand-free form of MIF and the MIF/compound **1** complex and the conformations of the residues in the active site are almost identical to that of previously reported structures.[13−18] Moreover, the crystal structures of the ligand-free form of MIF and the MIF/compound **1** complex can be superimposed for the Cα trace positions with an rmsd of 0.13 Å, and the active site residues in these structures (Pro-1, Met-2, Lys-32, Tyr-36, His-62, Ser-63, Ile-64, Tyr-95, Asn-97, Val-106, and Phe-113; the residues within 4 Å from compound **1**) can also be superimposed for non-hydrogen atoms of each of three active sites with rmsd of 0.22−0.53 Å. These indicate that major conformational changes do not occur upon the binding of compound **1**.

The omit electron-density map for compound **1** unambiguously revealed the orientation and conformation of the inhibitor in the active site of MIF (Figure 2). The ethyl ester portion of compound **1** and the side chain of neighboring Lys-32 show poor electron density, probably because of a multiple conformation in the crystal.

Structural Basis for Tautomerase Inhibition of MIF. Figure 3A,B shows the schematic representation of the interactions between compound **1** and MIF, and Figure 3C shows the stereoview of compound **1** in the active site of MIF.

Because the active site for tautomerization is located between two adjacent monomers, compound **1** interacts with two subunits. The 7-hydroxyl group forms a hydrogen bond with the carbonyl oxygen of the side chain of Asn-97. The backbone nitrogen of Ile-64 in MIF forms a bifurcated hydrogen bond with the 1-oxygen and the carbonyl oxygen at the 2-position of the coumarin ring of compound **1**. The hydroxyl group of Tyr-95 is too far from the carboxyl oxygen of the ester bond to form a hydrogen bond interaction (4.4 Å), though there may be a weak interaction between them. The secondary amine of Pro-1 is positioned above the ring of compound **1** which consists of O1−C4, C9, and C10, and the coumarin ring is located in the hydrophobic pocket which is formed by the side chains of Pro-1, Met-2, Ile-64, Tyr-95, Val-106, and Phe-113. These hydrogen bonds and hydrophobic interactions are thought to play a role in the binding of compound **1**. Similar interactions were also observed in the crystal structures of HPP/MIF and (*E*)-2-fluoro-*p*-hydroxycinnamate/MIF complexes.[17,18] In their structures, the ammonium groups of Lys-32 are located within hydrogen-bonding distance of the carboxyl oxygen of the ligands, but in our crystal structure, the ammonium group of the side chain of Lys-32 was disordered, though it was observed in the ligand-free form of MIF.

Figure 4 shows three superimpositions of compound **1** in the MIF/compound **1** complex into water molecules in three active sites of the ligand-free form of MIF. Good superimposition of two oxygen atoms of the carbonyl group at the 2-position and the 7-hydroxyl group of compound **1** on water molecules is observed, and in the crystal structure of the ligand-free form of MIF, the corresponding water molecules are located within hydrogen-bonding distance of the side chain of Asn-97 and the backbone amide of Ile-64. All of our hit compounds, except relatively low-potency compound **14** and compound **12**, have a hydroxyl group at the 7-position, and all except compound **13** have a carbonyl group at the 2-position. It seems that the positions which these two oxygen atoms of compound **1** occupy in the active site may be favorable for the hydrogen-bonding interactions to the target protein. The most potent compound, compound **13,** does not have a carbonyl group at the 2-position, but it has an oxygen atom at the 1-position which is expected to form a hydrogen bond to the backbone amide of Ile-64 (see below).

Second Hydrophobic Region at the Rim of the Active Site. Although the catalytic pocket of tautomerase in MIF which consists of Pro-1, Met-2, Ile-64, Tyr-95, Val-106, and Phe-113 is hydrophobic, our crystallographic study also revealed that there is a hydrophobic surface which consists of Pro-33, Tyr-36, Trp-108, and Phe-113 at the rim of the active site of MIF (Figure 3C). Because this second hydrophobic region is very close to the catalytic pocket, it is expected that the compounds which can span both the active site and the adjacent hydrophobic surface increase the binding affinity. The crystal structure of the MIF/compound **1** complex indicated that the substituent at the 3-position of the coumarin ring is thought to be located near the second hydrophobic region, though, unfortunately, the ethyl ester group of compound **1** was disordered in our structure. Figure 5A shows the docking model of compound **8** having a benzene ring at the 3-position of the coumarin ring. This model was obtained using DOCK4.0.1[25,26] in which the ligand-free form of MIF was used for the target receptor, and it showed that the benzene ring of compound **8** is stacked against the phenyl group of Tyr-36 in the second hydrophilic surface, without disrupting the binding of part of the coumarin ring. Compound **8** is a more potent compound than compound **1** (its K_i value is 0.47 μM),

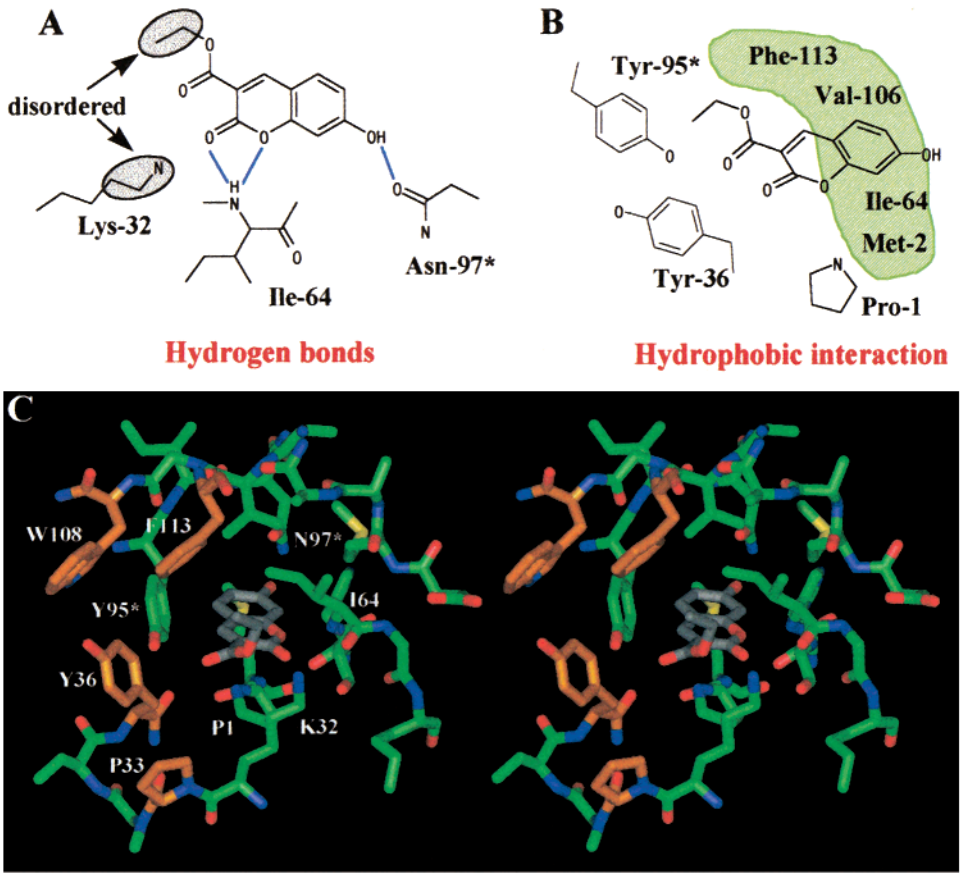

Figure 3. Schematic diagram, showing (A) the hydrogen bonds and (B) the intermolecular interactions between compound **1** and the surrounding residues of compound **1**. Hydrophobic pocket is green. (C) Stereoview of compound **1** positioned in the active site of MIF. The residues in the second hydrophobic surface at the rim of the active site are orange. Asterisk refers to an adjacent subunit.

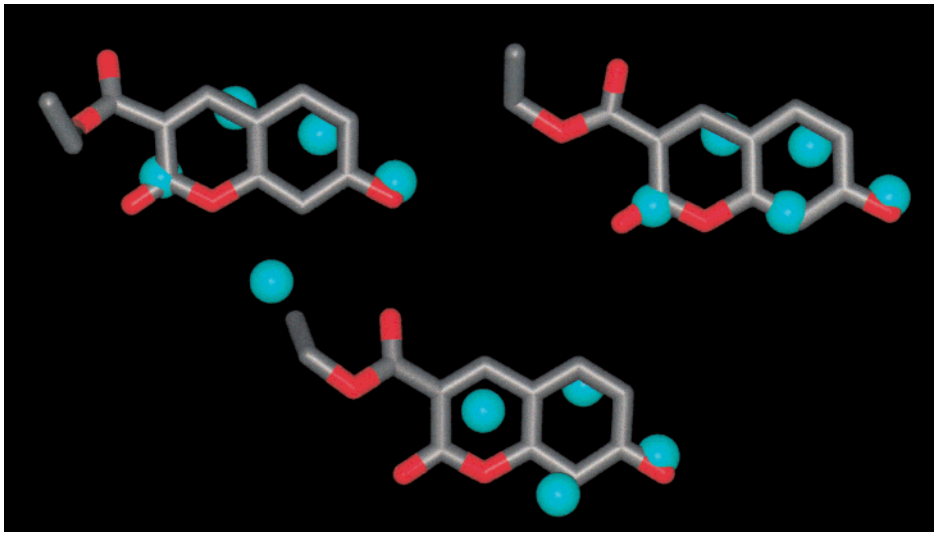

Figure 4. Superimposition of compound **1** in the MIF/compound **1** complex and water molecules (cyan) in each of three active sites of the ligand-free form of MIF.

and compounds **6**−**11**, having higher potency than compound **1**, also have aromatic rings at the 3-position of the coumarin ring. It seems that these hydrophobic interactions may contribute to their improved binding affinity. The distance between the carbonyl oxygen at the 2-position of compound **8** and the amine group of Lys-32 of MIF is 3.1 Å in our docking model, though in the crystal structure of MIF complexed with compound **1** the side chain of Lys-32 was disordered. Hydrogen bonding may occur between them.

Compound **13** (K_i = 0.038 μM) is the most potent tautomerase inhibitor of MIF we found. This compound is unique among our hit compounds, because it does not have a coumarin ring but has a chromen-4-one ring. Figure 5B shows the docking model of compound **13**. The rmsd between non-hydrogen atoms of the coumarin

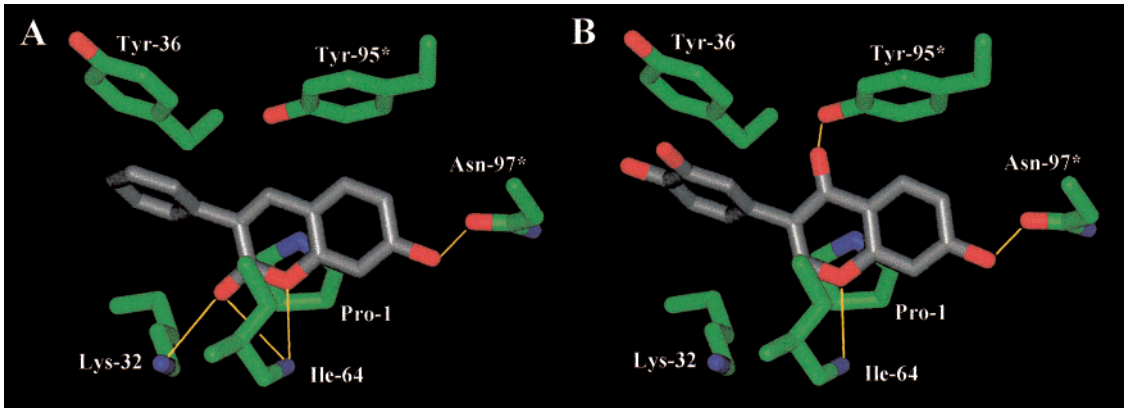

Figure 5. Results of docking of (A) compound **8** and (B) compound **13** into the active site of MIF. Yellow lines indicate hydrogen bonds.

ring of compound **1** in the crystal structure and the chromen-4-one ring of compound **14** in our model was 0.46 Å. As observed in the crystal structure of MIF complexed with compound **1**, the 7-hydroxyl group of compound **13** forms a hydrogen bond with the carbonyl oxygen of the side chain of Asn-97, and the 1-oxygen in the chromen-4-one ring forms a hydrogen bond with the backbone nitrogen of Ile-64. The benzene ring of cathechol is stacked against the phenyl group of Tyr-36 in the hydrophobic surface at the rim of the active site, as observed in compound **8**, while two hydroxyl groups of cathechol protrude into solvent. The most different feature of the interaction of compound **13** with the active site is that the carbonyl oxygen at the 4-position is located within hydrogen-bonding distance of the hydroxyl group of Tyr-95. (The distance between the carbonyl oxygen at the 4-position of compound **13** and the oxygen of the hydroxyl group of Tyr-95 of MIF is 2.5 Å in our docking model.) It seems that this postulated hydrogen bonding between compound **13** and the hydroxyl group of Tyr-95 may participate in its high affinity.

Structures of 14 Hit Compounds. On the basis of the structures, our 14 hit compounds are classified into four groups: (1) a 7-hydroxycoumarin group, (2) a coumarin group, (3) a 7-hydroxychromen-4-one group, and (4) a 7-hydroxychroman-2,4-dione group.

First, the 7-hydroxycoumarin group is the major group which consists of 11 compounds, compounds **1**−**11**. The crystal structure of compound **1** indicated that the hydroxyl group at the 7-position, the oxygen at the 1-position, and the carbonyl oxygen at the 2-position are critical for hydrogen bonding, and the coumarin ring hydrophobically interacts with the hydrophobic surface in the active site of MIF (Figure 3). Among the 524 compounds which were selected through the virtual screening approach, there were several coumarin derivatives which have a methoxy group at the 6- or 7-position. However, all such compounds showed no inhibition even at a concentration of 100 μM. The coumarin derivatives which have no substituents at the 6- and 7-positions also showed no inhibition except for compound **12** classified in the second group. It seems that these SARs (structure−activity relationships) support the importance of hydrogen bonding of the hydroxyl group at the 7-position. Because an amino group can also form a hydrogen bond, the inhibition assay of 7-aminocoumarin analogues was of interest; however, such compounds could not be obtained from commercial suppliers. Molecular modeling studies showed that the aromatic ring at the 3-position of the coumarin ring may interact with the hydrophobic surfaces at the rim of the active site (Figure 5). Among the 7-hydroxycoumarin group, there is a tendency for the compounds having an aromatic ring at the 3-position to show more potent inhibition.

In the second group, the coumarin group consists of compound **12**. Though this compound does not have a hydroxyl group at the 7-position, it showed a relatively good K_i value (1.6 μM). The substituent at the 3-position may be favorable for interaction with the hydrophobic surface at the rim of the active site. It is expected that the 7-hydroxycoumarin compounds having such a substituent at the 3-position would show higher inhibition, but they were also not commercially available.

Compound **13**, which belongs to the third 7-hydroxychromen-4-one group, is the most potent compound (K_i = 38 nM). A molecular modeling study showed that the oxygen at the 1-position, the carbonyl oxygen at the 4-position, and the hydroxyl group at the 7-position form hydrogen bonds and the cathechol part interacts with the hydrophobic surface at the rim of the active site (Figure 5B). Characteristic hydrogen bonding between the carbonyl oxygen at the 4-position and the hydroxyl group of Tyr-95 was not observed in any of the other crystal structures.[17,18] It seems that this hydrogen bond may play a role in the high affinity of compound **13**.

Compound **14**, which belongs to the last 7-hydroxychroman-2,4-dione group, does not have a hydroxyl group at the 7-position, but it also inhibited the tautomerase reaction (K_i = 6.2 μM). A molecular modeling study of compound **14** indicated that the carbonyl oxygen at the 4-position forms a hydrogen bond to the hydroxyl group of Tyr-95, as did compound **13** (data not shown). This hydrogen bond may compensate for the loss of the hydrogen bond of the hydroxyl group at the 7-position.

Catalytic Pocket of MIF. Because of the conserved N-terminal proline and structural similarity between MIF and two bacterial isomerases, 4-OT and CHMI, it was suggested that these proteins are also members of a superfamily.[16,35] On the basis of the crystal structure of 4-OT inactivated by an irreversible inhibitor, 2-oxo-3-pentynoate (2-OP), Taylor et al. proposed the mechanism of the isomerization of 4-OT.[36] In their mechanism, the secondary amine of Pro-1 acts as the general

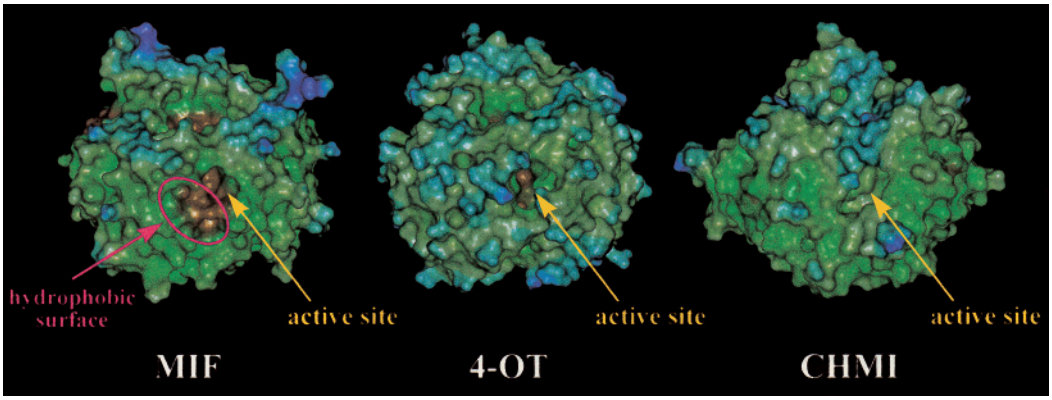

Figure 6. Comparison of surfaces of the lipophilicity potential of MIF, 4-OT, and CHMI. The color ramps for lipophilicity range from brown (highest lipophilic area of the protein) to blue (highest hydrophilic area). These surfaces were generated using SYBYL, MOLCAD module.

base, while the reaction intermediate is postulated to be stabilized by an ordered water molecule and the side chain of Arg-39 as a general acid catalyst. Because CHMI also has an arginine residue at the position corresponding to Arg-39 of 4-OT, as well as the conserved N-terminal proline, its isomerase mechanism is thought to be similar to that of 4-OT.[19]

The N-terminal proline is also conserved in MIF, and in the crystal structure of MIF complexed with HPP,[17] Pro-1 is located to function as a catalytic base. It was also reported that mutation of the N-terminal proline to glycine reduces the tautomerase activity and that the insertion of an alanine between Pro-1 and Met-2 essentially abolishes the activity.[17] However, MIF has a tyrosine residue (Tyr-95) at the position corresponding to Arg-39 of 4-OT, and in both crystal structures of MIF complexed with HPP[17] and (*E*)-2-fluoro-*p*-hydroxycinnamate,[18] Tyr-95 does not locate within the hydrogen-bonding distance of a ligand. However, because there are no other polar groups in the active site, it is thought that Tyr-95 may participate in the catalytic reaction.[18]

Our crystallographic study of the MIF/compound **1** complex revealed that the coumarin ring of compound **1** is located in the hydrophobic active site containing Pro-1 and Tyr-95. Though no hydrogen bonds of the secondary amine of Pro-1 and the hydroxyl group of Tyr-95 to compound **1** are observed in our crystal structure, these two hydrophobic residues seem to be important for the binding of the hydrophobic coumarin ring (Figure 3B,C). On the other hand, our molecular modeling study indicated that the carbonyl oxygen at the 4-position of the most potent compound **13** is located within the hydrogen-bonding distance of the hydroxyl group of Tyr-95 (Figure 5B). It is expected that a crystallographic study will reveal the existence of its hydrogen bond.

Our crystallographic study also revealed the existence of a second hydrophobic surface which consists of Pro-33, Tyr-36, Trp-108, and Phe-113 (Figure 3C), and our molecular modeling studies of compounds **13** and **8,** which are more potent compounds than compound **1**, showed the possibility of hydrophobic interactions between the aromatic rings at the 3-position of the chromen-4-one ring (coumarin ring) and the benzene ring of Tyr-36 (Figure 5). Figure 6 shows a comparison of the protein surfaces of MIF, OT-4, and CHMI. The surfaces are colored according to the lipophilicity potential, in which the hydrophobic regions are brown and the hydrophilic regions are blue. This shows that MIF has a hydrophilic surface and a second hydrophobic surface at the rim of the active site, while a similar hydrophobic region is not observed in both 4-OT and CHMI. Because this hydrophobic surface is observed only in MIF, it is expected that a specific potent inhibitor for MIF could be designed using the interaction with this region.

Conclusion

Through the virtual screening approach, we have identified 14 tautomerase inhibitors of MIF whose K_i values are in the range of 0.038−7.4 μM and also determined the crystal structure of MIF complexed with one of the hit compounds. Several tautomerase inhibitors of MIF, such as (*E*)-2-fluoro-*p*-hydroxycinnamate,[18] dopachrome analogues,[22] tryptophan derivatives,[23] and hexanethiol,[24] have been reported, but to our knowledge, our compounds are the most potent tautomerase inhibitors. It is not clear whether the tautomerase activity of MIF is linked to its physiological functions. However, it is expected that our study would benefit attempts to understand the biological functions of MIF and develop further therapeutic approaches related to MIF.

Experimental Section

Materials. All compounds were purchased from commercial suppliers and assayed without further purification. However, the structures of all 14 hit compounds were confirmed by ^{1}H NMR (400 or 500 MHz), ^{13}C NMR, and HRMS.

Docking Method and Selection of Compounds. We used the crystal structure solved in our laboratory at high resolution for the target receptor in the calculation of docking. About 1 000 000 compounds in the Available Chemicals Directory (ACD, Molecular Design Ltd. Information Systems) and the Available Chemicals Directory Screening Compounds (ACDSC, Molecular Design Ltd. Information Systems) were docked into the active site of MIF using DOCK4.0.1.[25,26] In the calculation, we did not dock the compounds whose number of heavy atoms is above 30, because the active site of MIF is not very large (Heavy_atoms_maximum, a parameter in DOCK4.0.1, was set to 30). After docking, we first selected about 5 000 compounds with high force field scores in three types of scoring functions of DOCK4.0.1: DOCK energy scoring, DOCK chemical scoring, and DOCK contact scoring. In the following step, unfavorable compounds, such as reagents, chemically unstable compounds, and the compounds which did not satisfy the condition of the rule-of-5[27] ((1) molecular weight 500, (2) number of hydrogen bond acceptors

10, (3) number of hydrogen bond donors 5, (4) calculated log *P* 5; three of the four conditions must be satisfied), were removed, using an in-house program. Finally, we selected 524 compounds by careful visual inspection in which the binding of the compound to the active site without protruding into the solvent and the hydrogen-bonding patterns were examined.

Hit compounds **1**−**12** and **14** were selcted from ACDSC (mdl number, compound **1**, MFCD00017641; compound **2**, MFCD00037480; compound **3**, MFCD00037379; compound **4**, MFCD00488460; compound **5**, MFCD00488326; compound **6**, MFCD00990393; compound **7**, MFCD00990394; compound **8**, MFCD00037574; compound **9**, MFCD01084670; compound **10**, MFCD00842152; compound **11**, MFCD00732679; compound **12**, MFCD00391941; compound **14**, MFCD00498480), and hit compound **13** was selcted from ACD (mdl number, compound **13**, MFCD00143002).

Expression and Purification. Recombinant MIF from human thymocytes was subcloned into *Nde*I and *Xho*I sites of the bacteriophage T7 expression plasmid pET22b (Novagen). His-tagged MIF was expressed in *Escherichia coli* BL21(DE3) (Novagen) for the crystallographic study, purified using metal affinity column Talon (Invitrogen) equilibrated with 125 mM sodium citrate in 10 mM Tris·HCl (pH 8.0) buffer, and eluted by additional 90 mM imidazole. Yield: about 250 mg of purified MIF trimer/L of growth.

Crystallization and Structure Determination. MIF was concentrated to about 100 mg/mL in crystallization buffer (14.4 mM β-mercaptoethanol, 0.1 mM PMSF, and 100 mM sodium citrate (pH 5.0)). Crystals of typical size 0.2 × 0.2 × 0.2 mm were obtained using the hanging drop vapor diffusion method by mixing equal volumes of protein and reservoir solution (0.6−1.5 M ammonium sulfate/0.1 M HEPES (pH 7.0)) at room temperature. For the inhibitor−complex structure analysis, the crystals were soaked in 10 mM compound **1**, 2.0 M ammonium sulfate, 15% glycerol and 0.1 M HEPES (pH 7.0) for 10 days before data collection. X-ray intensity data were collected at 100 K with synchrotron radiation at BL6B (Tsukuba Advanced Research Alliance) in the Photon Factory, National Laboratory for High Energy Accelerator Research Organization. Data were processed with DENZO[28] and scaled with SCALA[29] in CCP4. Crystallographic data for free-form and inhibited-form crystals are shown in Table 1.

The crystal structure of free-form MIF was determined by the molecular replacement method using the 2.6 Å structure of 1MIF in PDB as a starting model and refined to 1.5 Å resolution. The inhibitor was fitted into the electron density in the difference Fourier map calculated with the data for the inhibited-form crystal. Actually, since the quality of the inhibitor-omitted map in one binding site of MIF trimers was better than those in the other two, one inhibitor molecule was placed in this best site. The models of two other inhibitor molecules were then generated by referring to the conformation of the first molecule and the corresponding electron densities. The program X-PLOR[30] was used throughout these analysis and refinement processes, and the program O[31] was used to interpret the electron-density map. Coordinates have been deposited in the PDB (free form, 1GD0; inhibited form, 1GCZ).

Dopachrome Tautomerization Assay. For the inhibition study of tautomerase, D-dopachrome was used as the substrate of MIF. Fresh solutions of D-dopachrome were prepared by mixing a solution of D-DOPA (Sigma) in 10 mM sodium phosphate buffer (pH 6.0) containing 0.5 mM EDTA and the required volume of a solution of potassium periodate (Nacalai) to achieve a 1:2 molar ratio of D-dopachrome/periodate. The D-dopachrome solutions were prepared before the inhibition assay because of their relative instability.

The enzymatic activity of MIF was spectrophotometrically determined by monitoring the decrease in absorbance at 475 nm for 10 min. The total volume of the assay mixture was 200 μL, containing sodium phosphate buffer (pH 6.0) and an aliquot of MIF solution whose final concentration was 4 μg/mL. Each inhibitor was added to the assay mixtures with 2 μL DMSO solution (final concentration of DMSO was 1% (v/v)). We determined that no inhibition of enzymatic activity by DMSO was observed at this concentration. The assay was initiated by the addition of the substrate ranging from 0.25 to 0.5 mM. All initial rates were corrected for background by performing an assay at the each substrate and inhibitor concentration without MIF and subtracting the uncatalyzed rate from the initial rate in the present of MIF. K_i values were determined using three-dimensional nonlinear regression analysis.

Acknowledgment. We thank N. Watanabe, M. Suzuki, and N. Igarashi, High Energy Accelerator Research Organization, for help in data collection at Photon Factory. N.K. and H.K. are members of the SBSP (Structural Biology Sakabe Project) of FAIS (Foundation for Advancement of International Science).

References

(1) Bloom, B. R.; Bennett, B. Mechanism of a reaction in vitro associated with delayed-type hypersensitivity. *Science* **1966**, *153*, 80−82.
(2) David, J. R. Delayed hypersensitivity in vitro: its mediation by cell-free substances formed by lymphoid cell-antigen interaction. *Proc. Natl. Acad. Sci. U.S.A.* **1966**, *56*, 72−77.
(3) Bernhagen, J.; Calandra, T.; Mitchell, R. A.; Martin, S. B.; Tracey, K. J.; Voelter, W.; Manogue, K. R.; Cerami, A.; Bucala, R. MIF is a pituitary-derived cytokine that potentiates lethal endotoxaemia. *Nature* **1993**, *365*, 756−759.
(4) Calandra, T.; Bernhagen, J.; Metz, C. N.; Spiegel, L. A.; Bacher, M.; Donnely, T.; Cerami, A.; Bucala, R. MIF as a glucocorticoid-induced modulator of cytokine production. *Nature* **1995**, *377*, 68−71.
(5) Bacher, M.; Metz, C. N.; Calandra, T.; Mayer, K.; Chesney, J.; Lohoff, M.; Gemsa, D.; Donnely, T.; Bucala, R. An essential regulatory role for macrophage migration inhibitory factor in T-cell activation. *Proc. Natl. Acad. Sci. U.S.A.* **1996**, *93*, 7849−7854.
(6) Calandra, T.; Spiegel, L. A.; Metz, C. N.; Bucala, R. Macrophage migration inhibitory factor (MIF) is a critical mediator of the activation of immune cells by exotoxins of Gram-positive bacteria. *Proc. Natl. Acad. Sci. U.S.A.* **1998**, *95*, 11383−11388.
(7) Donnely, S. C.; Bucala, R. Macrophage migration inhibitory factor: a regulator of glucocorticoid activity with a critical role in inflammatory disease. *Mol. Med. Today* **1997**, *3*, 502−507.
(8) Mikulowska, A.; Metz, C. N.; Bucala, R.; Holmdahl, R. Macrophage migration inhibitory factor is involved in the pathogenesis of collagen type II-induced arthritis in mice. *J. Immunol.* **1997**, *158*, 5514−5517.
(9) Leech, M.; Metz, C. N.; Santos, L.; Peng, T.; Holdsworth, S. R.; Bucala, R.; Morand, E. F. Involvement of macrophage migration inhibitory factor in the evolution of rat adjuvant arthritis. *Arthritis Rheum.* **1998**, *41*, 910−917.
(10) Lan, H. Y.; Bacher, M.; Yang, N.; Mu, W.; Nikolic-Paterson, D. J.; Metz, C.; Meinhardt, A.; Bucala, R.; Atkins, R. C. The pathogenic role of macrophage migration inhibitory factor in immunologically induced kidney disease in the rat. *J. Exp. Med.* **1997**, *185*, 1455−1465.
(11) Lan, H. Y.; Yang, N.; Brown, F. G.; Isbel, N. M.; Nikolic-Paterson, D. J.; Mu, W.; Metz, C. N.; Bacher, M.; Atkins, R. C.; Bucala, R. Macrophage migration inhibitory factor expression in human renal allograft rejection. *Transplantation* **1998**, *66*, 1465−1471.
(12) Bozza, M.; Satoskar, A. R.; Lin, G.; Lu, B.; Humbles, A. A.; Gerard, C.; David, J. R. Targeted disruption of migration inhibitory factor gene reveals its critical role in sepsis. *J. Exp. Med.* **1999**, *189*, 341−346.
(13) Sun, H.-W.; Bernhagen, J.; Bucala, R.; Lolis, E. Crystal structure at 2.6-Å resolution of human macrophage migration inhibitory factor. *Proc. Natl. Acad. Sci. U.S.A.* **1996**, *93*, 5191−5196.
(14) Suzuki, M.; Sugimoto, H.; Nakagawa, A.; Tanaka, I.; Nishihira, J.; Sakai, M. Crystal structure of the macrophage migration inhibitory factor from rat liver. *Nat. Srtuct. Biol.* **1996**, *3*, 259−266.
(15) Sugimoto, H.; Suzuki, M.; Nakagawa, A.; Tanaka, I.; Nishihira, J. Crystal structure of macrophage migration inhibitory factor from human lymphocyte at 2.1 Å resolution. *FEBS Lett.* **1996**, *389*, 145−148.
(16) Stamps, S. L.; Fitzgerald, M. C.; Whitman, C. P. Characterization of the role of the amino-terminal proline in the enzymatic activity catalyzed by macrophage migration inhibitory factor. *Biochemistry* **1998**, *37*, 10195−10202.

(17) Lubetsky, J. B.; Swope, M.; Dealwis, C.; Blake, P.; Lolis, E. Pro-1 of macrophage migration inhibitory factor functions as a catalytic base in the phenylpyruvate tautomerase activity. *Biochemistry* **1999**, *38*, 7346−7354.
(18) Taylor, A. B.; Johnson, Jr., W. H.; Czerwinski, R. M.; Li H.-S.; Hackert, M. L.; Whitman, C. P. Crystal structure of macrophage migration inhibitory factor complexed with (*E*)-2-fluoro-*p*-hydroxycinnamate at 1.8 Å resolution: Implications for enzymatic catalysis and inhibition. *Biochemistry* **1999**, *38*, 7444−7452.
(19) Subramanya, H. S.; Roper, D. I.; Dauter, Z.; Dodson, E. J.; Davies, G. J.; Wilson, K. S.; Wigley, D. B. Enzymatic ketonization of 2-hydroxymuconate: Specificity and mechanism investigated by the crystal structures of two isomerases. *Biochemistry* **1996**, *35*, 792−802.
(20) Rosengren, E.; Bucala, R.; Arnan, P.; Jacobsson, L.; Odh, G.; Metz, C. N.; Rorsman, H. The immunoregulatory macrophage migration inhibitory factor (MIF) catalyzes a tautomerization reaction. *Mol. Med*. **1996**, *2*, 143−149.
(21) Rosengren, E.; Aman, P.; Thelin, S.; Hansson, C.; Ahlfors, S.; Bjork, P.; Jacobsson, L.; Rorsman, H. The macrophage migration inhibitory factor MIF is a phenylpyruvate tautomerase. *FEBS Lett.* **1997**, *417*, 85−88.
(22) Zhang, X.; Bucala, R. Inhibition of macrophage migration inhibitory factor (MIF) tautomerase activity by dopachrome analogues. *Bioorg. Med. Chem. Lett.* **1999**, *9*, 3193−3198.
(23) Al-Abed, Y.; Dios, A.; Mitchell, R.; Metz, C.; Bucala, R. Chemical approach toward inhibiting MIF bioactivity. American Chemical Society 219th National Meeting, San Francisco, CA, 2000; Abstr. MEDI 287.
(24) Swope, M. D.; Sun, H.-W.; Klockow, B.; Blake, P.; Lolis, E. Macrophage migration inhibitory factor interactions with glutathione and S-hexylglutathione. *J. Biol. Chem*. **1998**, *273*, 14877−14884.
(25) Kuntz, I. D. Structure-based strategies for drug design and discovery. *Science* **1992**, *257*, 1078−1082.
(26) Shoichet, B. K.; Stroud, R. M.; Santi, D. V.; Kuntz, I. D.; Perry, K. M. Structure-based discovery of inhibitors of thymidylate synthase. *Science* **1993**, *259*, 1445−1450.
(27) Lipinski, C. A.; Lombardo, F.; Dominy, B. W.; Feeney, P. J. Experimental and computational approaches to estimate solubility and permeability in drug discovery and development settings. *Adv. Drug Deliv. Rev.* **1997**, *23*, 3−25.
(28) Otwinowski, Z. In *Oscillation data reduction program*; Sawyer, L., Isaaca, N., Burley, S., Eds.; CCP4 Study Weekend; SERC Daresbury Laboratory: Daresbury, U.K., 1993; pp 56−62.
(29) The CCP4: A Suite of Programs for Protein Crystallography. *Acta Crystallogr.* **1994**, *D50*, 760−763.
(30) Brunger, A. T. *XPLOR Manual*; Yale University Press: New Haven, CT, 1992.
(31) Jones, T. A.; Zou, J. Y.; Cowan, S. W.; Kjeldgaard, M. Improved methods for binding protein models in electron density maps and the location of errors in these models. *Acta Crystallogr. A* **1991**, *47*, 110−119.
(32) Sarmiento, M.; Wu, L.; Keng, Y.-F.; Song, Li.; Luo, Z.; Huang, Z.; Wu, G.-Z.; Yuan, A. K.; Zhang, Z.-Y. Structure-based discovery of small molecule inhibitors targeted to protein tyrosine phosphatase 1B. *J. Med. Chem*. **2000**, *43*, 146−155.
(33) Charifson, P. S.; Corkery, J. J.; Murcko, M. A.; Walters, W. P. Consensus scoring: A method for obtaining improved hit rates from docking databases of three-dimensional structures into proteins. *J. Med. Chem*. **1999**, *42*, 5100−5109.
(34) Massova, I.; Martin, P., Bulychev, A.; Kocz, R.; Doyle, M.; Edwards, B. F. P.; Mobashery, S. Templates for design of inhibitors for serine proteases: Application of the program DOCK to the discovery of novel inhibitors for thrombin. *Bioorg. Med. Chem. Lett.* **1998**, *8*, 2463−2466.
(35) Murzin, A. G. Structural classification of proteins: new superfamilies. *Curr. Opin. Struct. Biol.* **1996**, *6*, 386−394.
(36) Taylor, A. B.; Czerwinski, R. M.; Johnson, W. H., Jr.; Whitman, C. P.; Hackert, M. L. Crystal structure of 4-oxalocrotonate tautomerase inactivated by 2-oxo-3-pentynoate at 2.4 Å resolution: Analysis and implications for the mechanism of inactivation and catalysis. *Biochemistry* **1998**, *37*, 14692−14700.

JM000386O